Magnetic ground states of $CaRu_{1-x}Mn_xO_3$ ($0.2 \leq x \leq 0.9$): a magnetic Compton scattering study

2009 J. Phys.: Condens. Matter 21 276003

(http://iopscience.iop.org/0953-8984/21/27/276003)

J. Phys.: Condens. Matter **21** (2009) 276003 (6pp) doi:10.1088/0953-8984/21/27/276003

Magnetic ground states of $CaRu_{1-x}Mn_xO_3(0.2 \leqslant x \leqslant 0.9)$: a magnetic Compton scattering study

S Mizusaki[1,7], T Taniguchi[1], N Okada[1], Y Nagata[1], N Hiraoka[2], M Itou[3], Y Sakurai[3], Y Noro[4], T C Ozawa[5] and H Samata[6]

[1] College of Science and Engineering, Aoyama Gakuin University, Fuchinobe, Sagamihara, Kanagawa 157-8572, Japan
[2] National Synchrotron Radiation Research Center, Hsin-Ann Road, Hsinchu Science Park, Hsinchu 30076, Taiwan, Republic of China
[3] Japan Synchrotron Radiation Research institute (JASRI/SPring-8), Sayo, Hyogo 679-5198, Japan
[4] Kawazoe Frontier Technologies, Co. Ltd, Kuden, Sakae, Yokohama, Kanagawa 931-113, Japan
[5] Nanoscale Materials Center, National Institute for Materials Science, Namiki, Tsukuba, Ibaraki 305-0044, Japan
[6] Faculty of Maritime Sciences, Kobe University, Fukaeminami, Higashinada, Kobe, Hyogo 658-0022, Japan

E-mail: smizusaki@ee.aoyama.ac.jp

Received 24 December 2008, in final form 27 May 2009
Published 12 June 2009
Online at stacks.iop.org/JPhysCM/21/276003

Abstract

The magnetism of $CaRu_{1-x}Mn_xO_3(0.2 \leqslant x \leqslant 0.9)$ was studied by the magnetic Compton scattering experiment. The result of the spin-polarized electron momentum density distributions (magnetic Compton profiles) and the absolute value of spin moment indicate that Mn doping introduces magnetic moments on Ru ions, and the Ru and Mn spin moments were antiferromagnetically coupled. Moreover the spin moment of Ru ions increased proportionally in the x range. These results were explained by a mixed valence model and inhomogeneous magnetic structure, where the inhomogeneous magnetic ground state in $CaRu_{1-x}Mn_xO_3$ would be formed by a ferrimagnetic network from the $Mn^{3.5+}$ and $Ru^{4.5+}$ clusters in the paramagnetic matrix $CaRuO_3$ for $x < 0.5$ and in the antiferromagnetic matrix $CaMnO_3$ for $x > 0.5$.

1. Introduction

Perovskite-type ruthenium oxides $MRuO_3$ (M = Sr, Ca) have attracted much attention because of their interesting magnetic and transport properties. While $SrRuO_3$ is a ferromagnet with a Curie temperature T_C of 160 K, $CaRuO_3$ is considered to be an itinerant paramagnet with antiferromagnetic characteristics since magnetization measurements have shown a Weiss temperature of −200 K [1, 23]. Both compounds possess a $4d^4$ low spin configuration ($S = 2/2$) on Ru and are thought to have a narrow itinerant band made by the hybridization of Ru $4d$ t_{2g} and O $2p$ orbitals [2–4]. It has been reported that ferromagnetism appears in $CaRuO_3$ by substituting Ru ions for other magnetic or non-magnetic ions [19], such as Ti [5, 19], Mn [6–13, 19], Fe [14–17, 19], Co [18], Ni, Rh [2] and Sn [3]. The intraband electron–electron interactions and electron–phonon couplings play an important role in such narrow $4d$-band systems, and a slight change in the interactions or couplings may cause the transition from itinerant to localized electron systems, associated with a remarkable change of the magnetic properties.

$CaRu_{1-x}Mn_xO_3$ is a ferromagnet with a relatively large magnetic moment and a high Curie temperature T_C, compared to ferromagnetic $SrRuO_3$. Interestingly, the ferromagnetism appears in a wide x range between itinerant paramagnetic $CaRuO_3$ and localized antiferromagnetic $CaMnO_3$ [8–10]. An x-ray magnetic circular dichroism measurement of epitaxially

[7] Author to whom any correspondence should be addressed.

grown $CaMn_{1-x}Ru_xO_3$ thin films revealed that the Mn and Ru spin moments are aligned antiparallel [12]. Neutron diffraction and x-ray absorption measurements of $CaMn_{0.6}Ru_{0.4}O_3$ showed the existence of Ru^{5+} [13]. Our previous paper presented an anomalous change in the unit cell volume and discussed the magnetic properties on the basis of the mixed valence model with $Mn^{3+}(3d^4)$, $Mn^{4+}(3d^3)$, $Ru^{4+}(4d^4)$ and $Ru^{5+}(4d^3)$ ions [10]. The model assumes antiferromagnetic coupling between the Ru and Mn spins and is reasonably consistent with other experimental results. An additional investigation is necessary to clarify the magnetic ground states of the $CaRu_{1-x}Mn_xO_3$ system for examining the validity of the assumption. In this work, we have obtained the Ru and Mn spin moments of $CaRu_{1-x}Mn_xO_3(0.2 \leqslant x \leqslant 0.9)$ using the MCS technique in order to clarify the magnetic ground states of the system.

Magnetic Compton scattering (MCS) is a powerful tool to discuss the magnetic ground states of ferro- and ferrimagnetic materials through magnetic spin moment and the electronic structure of materials [20, 21] because the MCS samples only the spin moment, μ_S, and provides a magnetic Compton profile (MCP), $J_{mag}(p_z)$. The orbital moment, μ_L, is yielded without the necessity of a theoretical model by comparison with bulk magnetization measurement. Moreover, the MCS permit us to test the theoretical model through the Compton profiles. Since the momentum wavefunction is related to the real-space wavefunction via a Fourier transform, the shape of CP intrinsically includes information about the overall electron momentum.

Experimentally, the Compton profile, $J(p_z)$ is provided by the energy spectrum of Compton-scattered x-rays as the one-dimensional projection of ground-state electron momentum density for all electrons in materials. The electron momentum, $\boldsymbol{p}$, is represented by an atomic unit (au). One atomic unit of momentum is 1.99×10^{-24} kg m s^{-1}. However, it is impossible for this method to distinguish the two magnetic species and the site component. But CP can be decomposed into a few partial electron orbital profiles for s, p, d and f electrons because these electron orbitals have a different electron momentum distribution. Since the scattering cross section contains a spin-dependent component, extraction of the spin-dependent component is performed by taking a difference between two Compton profiles measured with a magnetic field parallel or antiparallel to the scattering vector using a circularly polarized incident x-rays. The difference in two Compton profiles is called the magnetic Compton profile, MCP: $J_{mag(p_z)}$. Theoretically, MCP is defined as the one-dimensional projection of the spin-polarized electron momentum density:

$$J_{mag}(p_z) = \int\int [n^{\uparrow}(\boldsymbol{p}) - n^{\downarrow}(\boldsymbol{p})]\,\mathrm{d}p_x\,\mathrm{d}p_y,$$

where $n^{\uparrow}(\boldsymbol{p})$ and $n^{\downarrow}(\boldsymbol{p})$ are the momentum densities of the majority and minority spin bands, respectively [20, 21]. The area under the MCP is equal to the total spin moment (μ_{spin}) per formula unit (f.u.):

$$\int_{-\infty}^{+\infty} J_{mag}(p_z)\,\mathrm{d}p_z = \mu_{spin}.$$

2. Experimental details

The MCS experiment was carried out at the BL08W beamline of SPring-8. The sample temperature was 10 K and the applied magnetic field was 2.5 T. The overall momentum resolution was 0.57 atomic units (au). The details of the experiment are described in previous papers [4, 16, 20, 21, 24]. The procedures of the standard data analysis were employed and the experimental MCPs were folded at zero momentum to increase the statistical accuracy after confirming the symmetrical shape of the MCPs with respect to zero momentum. A standard Fe sample, in which the spin moment was already known, was measured in order to normalize the experimental MCPs of $CaRu_{1-x}Mn_xO_3$ to the total spin moments per formula unit.

The samples in this study were the same as in the previous paper [10]. We confirmed that each of the prepared samples is a single phase. Polycrystalline samples of $CaRu_{1-x}Mn_xO_3(0.2 \leqslant x \leqslant 0.9)$ were prepared by the solid-state reaction method using high-purity reagents of $CaCO_3$ (99.9%), Ru metal (99.9%) and Mn_2O_3 (99.9%). The chemical composition and homogeneity were characterized by electron-probe microanalysis (EPMA) using wavelength-dispersive spectrometers. The crystal structure was characterized at room temperature by x-ray powder diffraction (XRD) using Cu Kα radiation, and the structural parameters were obtained by refinement using the Rietveld method.

Ab initio restricted Hartree–Fock (RHF) molecular orbital calculations were performed for RuO_6 and MnO_6 clusters using the GAMESS program [22] to obtain the theoretical Ru $4d$ and Mn $3d$ Compton profiles. The clusters were embedded in point charges that describe the Madelung potentials [24]. The ionic valences of Ca, Ru, Mn and O ions were assumed to be $2+$, $4+$, $4+$ and $2-$, respectively. The structural parameters determined by the XRD measurements were used for the calculations.

3. Results and discussion

The XRD patterns show that all of the $CaRu_{1-x}Mn_xO_3$ samples have a single phase of $GdFeO_3$-type orthorhombic perovskite structure. Figure 1 shows the lattice parameters of the refined structures as a function of Mn concentration. This refinement shows that the Ru and Mn ions were distributed on the same site. Figure 2 displays all the experimental MCPs, together with the best fits of theoretical Ru $4d$ and Mn $3d$ profiles into the experiments. Table 1 shows the spin moments S and magnetizations J at 10 K under a magnetic field of 2.5 T, where the spin moments are determined from the MCS intensities. The estimation errors were $\sim$0.002 μ_B. The last column presents the orbital moments $L(=J - S)$, and the orbital moment is almost quenched in the system. The spin moments are smaller than the values estimated from Ru and Mn ions with the low spin configurations, probably due to unsaturated magnetizations.

Figure 3 presents the MCPs of $Ca_{0.5}Sr_{0.5}RuO_3$ and $CaRu_{0.5}Mn_{0.5}O_3$, together with the calculated RHF profiles of Ru $4d$ and Mn $3d$ states to show how the MCP reflects the spin-polarized electronic states. The spin moment of

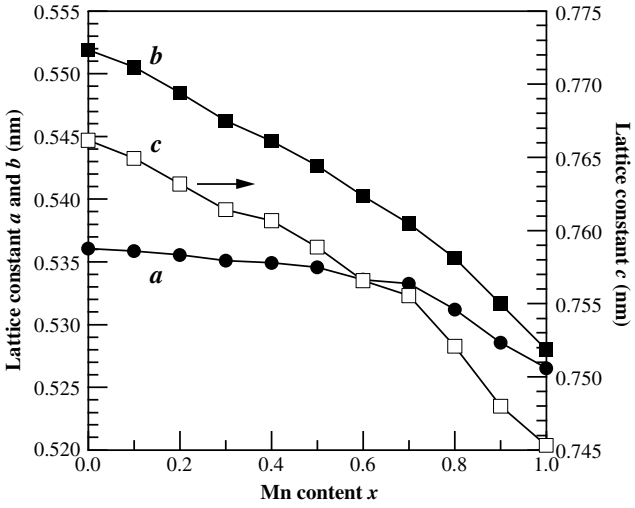

Figure 1. Lattice parameters of $CaRu_{1-x}Mn_xO_3$ at room temperature [10].

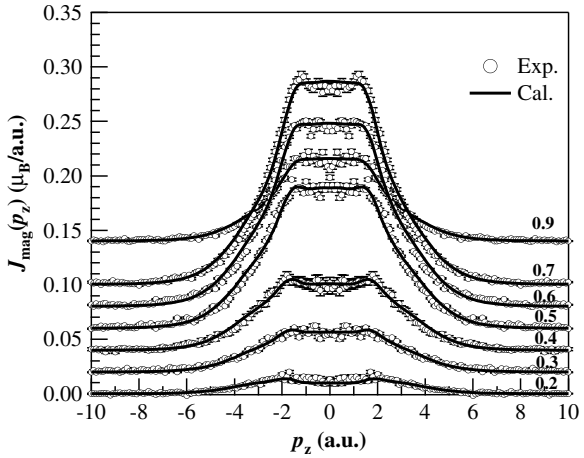

Figure 2. Experimental magnetic Compton profiles (open circles) of $CaRu_{1-x}Mn_xO_3$ at 10 K under 2.5 T and theoretical ones obtained by best fits using calculated RHF Compton profiles of Mn 3*d* and Ru 4*d* states (solid lines).

Table 1. Experimental spin moment S, magnetization J, and the difference (orbital moment) $J - S$ at 10 K under a field of 2.5 T.

x (Mn)	Spin moment: S (μ_B/f.u.)	Magnetization: J (μ_B/f.u.)	$J - S$ (μ_B/f.u.)
0.9	0.456	0.439	−0.017
0.7	1.14	1.12	−0.02
0.5	0.869	0.778	−0.091
0.3	0.277	0.223	−0.054
0.2	0.108	0.087	−0.021

$Ca_{0.5}Sr_{0.5}RuO_3$ is carried mostly by the Ru 4*d* state, and thus the overall shape of its MCP was reproduced well by the calculated RHF Ru 4*d* profile (see figure 3(a)). The slight discrepancy found around $p_z = 0$ was explained by the effect of hybridization between the Ru 4*d* and O 2*p* orbitals [24]. On the other hand, the MCP of $CaRu_{0.5}Mn_{0.5}O_3$ was not reproduced by a single profile of the calculated RHF

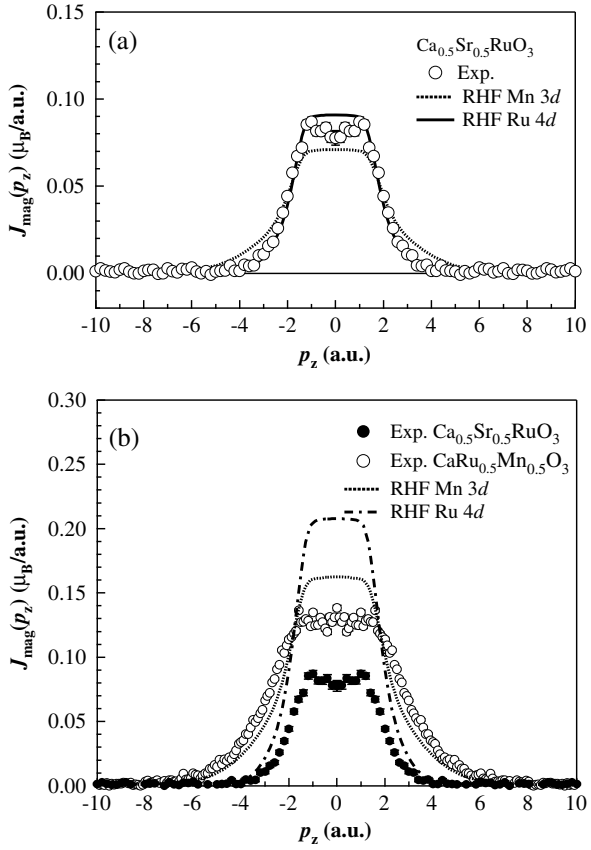

Figure 3. Experimental magnetic Compton profile of (a) $Ca_{0.5}Sr_{0.5}RuO_3$ and (b) $CaRu_{0.5}Mn_{0.5}O_3$, together with the calculated RHF profiles of Mn 3*d* and Ru 4*d* states. The area under the experimental and calculated profiles was normalized to the value of the spin moment.

Ru 4*d* nor Mn 3*d* state (see figure 3(b)). It is clear that the MCP of $CaRu_{0.5}Mn_{0.5}O_3$ was different from the experimental ferromagnetic Ru 4*d* profile of $Ca_{0.5}Sr_{0.5}RuO_3$. The difference between them means that the Mn 3*d* moment is dominant for the spin moment of $CaRu_{0.5}Mn_{0.5}O_3$ and therefore both Ru 4*d* and Mn 3*d* states were spin-polarized in this compound.

Figure 4 shows the best fit with the RHF profiles in the experimental MCP, indicating that the Mn 3*d* dominated the spin moment and the Mn and Ru spin moments were coupled antiferromagnetically. The antiferromagnetic coupling is probably caused by the superexchange interaction via O 2*p* orbitals [16, 25].

The experimental results of spin moment and decomposition by the shape analysis of the present magnetic Compton scattering are summarized in figure 5, which shows the Ru 4*d* and Mn 3*d* spin moments as well as the total spin moment in $CaRu_{1-x}MnO_3 (0.2 \leqslant x \leqslant 0.9)$. The Ru and Mn spin moments were obtained from the combination between the total spin moments and the result of the profile shape analysis by best fits with calculated RHF profiles. Figure 5 shows that, although Ru ions in $CaRuO_3$ are non-magnetic, Mn doping induced the spin moment on the Ru site, the Mn ions dominated the spin moment and the Ru spin moment was antiparallel to the Mn spin moments in the x range between 0.2 and 0.9. Interestingly, the magnetic moment with respect to x is different

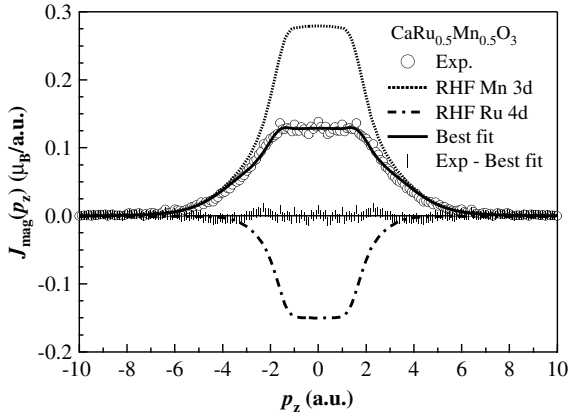

Figure 4. Experimental magnetic Compton profile (open circle) of $CaRu_{0.5}Mn_{0.5}O_3$ at 10 K under 2.5 T and the best fit with calculated RHF Compton profiles (solid line) of Mn 3*d* and Ru 4*d* states into the experiment. The one-dot chain line and the broken line are the calculated RHF Compton profiles for Mn 3*d* and Ru 4*d* electrons, respectively.

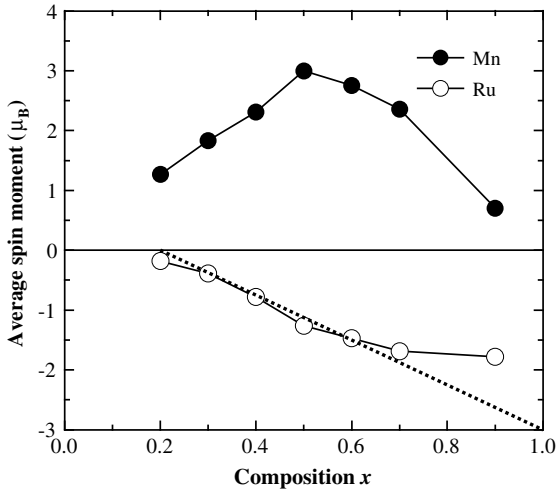

Figure 6. Mn composition dependence of the average spin moment per Ru or Mn ion in $CaRu_{1-x}Mn_xO_3$. The broken line shows the extrapolation of the data between $x = 0.2$ and 0.6 towards $x = 1.0$.

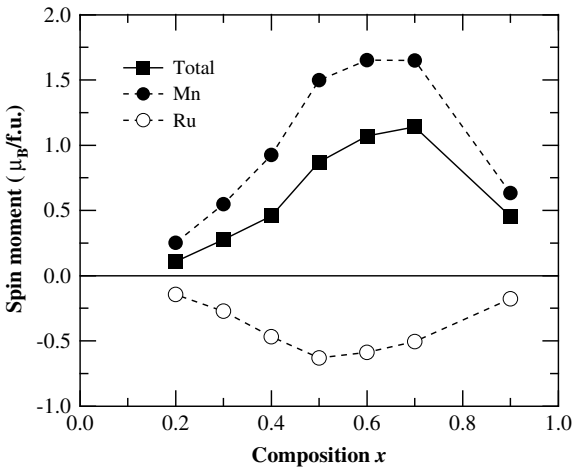

Figure 5. Total spin moment, and decomposed Mn and Ru spin moments for $CaRu_{1-x}Mn_xO_3$ as a function of the Mn composition x. The values were given in Bohr magneton per formula unit (μ_B/f.u.).

from that of the $CaRu_{1-x}Fe_xO_3$ system, in which Ru dominates the spin moment [16]. While the total and Mn spin moments had their maxima at $x = 0.7$, the Ru spin moment has its maximum at $x = 0.5$. The spin moments for $x = 0.5$ were $+1.499$ μ_B/f.u. for Mn 3*d* and -0.630 μ_B/f.u. for Ru 4*d*, which indicates that the average spin moments per ion are ~ 3 μ_B for Mn and ~ 1.5 μ_B for Ru. The average spin moment per ion for Mn was consistent with the theoretical moment of the Mn^{4+} ion and that for Ru is close to the value in $SrRuO_3$ [26].

Figure 6 plotted the average spin moments per ion for Mn 3*d* and Ru 4*d* calculated from the result of figure 5. The plot shows that the Mn moment was a maximum at $x = 0.5$. On the other hand, the Ru moment increased linearly from 0 to 0.169 μ_B for $x = 0.7$. The extrapolation value of 3 μ_B at $x = 1.0$ for average Ru moment is almost the same as the value of 2.8 μ_B per Ru^{5+} ion in Ba_2HoRuO_6, which is determined by neutron diffraction at 10 K [27]. This fact suggests that Ru^{5+} ions may contribute to align the spin moment on the Ru site in $CaRu_{1-x}MnO_3$, while Ru^{4+} ions are thought to be paramagnetic. The saturation of the Ru spin moment above $x = 0.7$ would be likely due to the formation of a canted or antiferromagnetic configuration on the Ru sublattice under the influence of the growing antiferromagnetic order of the Mn sublattice. The average spin moment for Mn 3*d* increases from 1.2 μ_B at $x = 0.2$ to 3 μ_B at $x = 0.5$, and then it decreases monotonically down to 0.7 μ_B at $x = 0.9$. The monotonic decrease is presumably due to the increase of the antiferromagnetic order of Mn ions since the end member at $x = 1.0$, $CaMnO_3$, has an antiferromagnetic order of Mn^{4+} ions.

The present experimental results suggest that $CaRu_{1-x}Mn_xO_3$ would be magnetically inhomogeneous under the mixed valence states of Ru and Mn ions. If it is homogeneous and both ions were in single valence states, the average spin moment per ion should be almost constant over the whole x range. However, the experiment shows the x dependence (see figure 6), i.e. the Mn spin moment shows its maximum at $x = 0.5$ and the Ru spin moment has the monotonic increase.

Figure 7 displays the relationship in the average spin moments between the Ru and Mn ions. A good linear relationship was shown between the Ru and Mn spin moments. Its slope was approximately 0.5, which is equivalent to the induction of spin moment for ~ 1.5 μ_B on Ru ions and 3 μ_B on Mn ions. This indicates that both Ru and Mn ions have their full spin moments for $x = 0.5$. Moreover, this linear relationship indicates that a single coupling mechanism would exist between the Ru and Mn spin moments, and the mechanism of ferrimagnetism could be described on the basis of the localized electron system. Therefore, a single scenario can describe to explain the magnetic properties in $CaRu_{1-x}Mn_xO_3$, as follows.

One possible explanation for the x dependence is the existence of two different regions with different magnetic

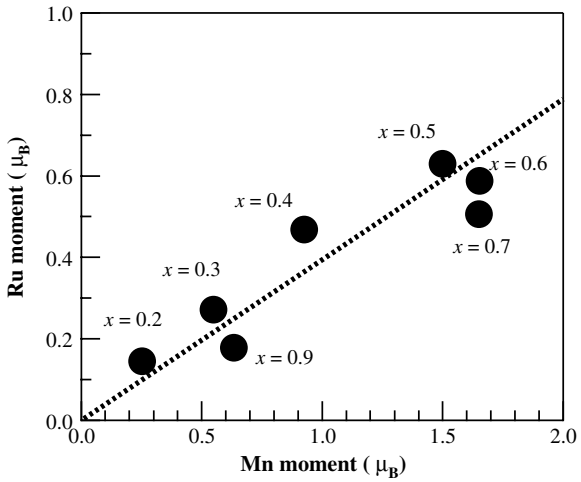

Figure 7. Relationship between the experimental spin moments of Mn and Ru ions in $CaRu_{1-x}Mn_xO_3$. The dotted lines are guides to the eyes.

ground states before and after $x = 0.5$. Region I below $x = 0.5$ is a mix of paramagnetic and ferrimagnetic states and region II above $x = 0.5$ is that of antiferromagnetic and ferrimagnetic states. At the border ($x = 0.5$), a single ferrimagnetic phase would appear with an almost perfect ferromagnetic order each in the Ru and Mn sublattices.

In short, region I is a magnetically inhomogeneous system, which consists of the ferrimagnetic Mn–Ru networks and paramagnetic Ru domains ($CaRuO_3$ matrix). The magnetism of ferrimagnetic Mn–Ru networks might be described by the localized electron system, although the present result could not identify whether the paramagnetic Ru^{4+} ions in the $CaRuO_3$ matrix belong to the itinerant or localized electron system. The suggested mechanism is as follows. In region I, doped Mn ions would be in a mixed valence state of Mn^{3+}–Mn^{4+}. The Mn^{3+}–Mn^{4+}(=$Mn^{3.5+}$) pairs are ferromagnetic due to the superexchange interaction between $Mn^{3+}(d^4)$ and $Mn^{4+}(d^3)$ ions [24], while isolated Mn^{3+} and Mn^{4+} ions do not show any ferromagnetic order. As the Mn composition increases, the number of Mn^{3+}–Mn^{4+} pairs increases and thus the average spin moment of Mn ions increases. As the number of Mn^{3+} ions increases, the number of Ru^{5+} ions increases to maintain charge neutrality. Then the number of Ru^{4+}–Ru^{5+}($Ru^{4.5+}$) pairs would increase. The $Ru^{4.5+}$ pairs would be ferromagnetic due to superexchange interaction and, as a result, the average spin moment of Ru ions increases as the Mn composition increases. Then, a group of the $Mn^{3.5+}$ and $Ru^{4.5+}$ pairs created a ferrimagnetic network, in which the Mn and Ru spin moments are coupled antiferromagnetically due to the antiferromagnetic superexchange interaction. In other parts, where such networks are not developed, the Ru ions remain paramagnetic.

Region II would be a magnetically inhomogeneous system in which the antiferromagnetic Mn–Mn ($CaMnO_3$ matrix) and ferrimagnetic Ru–Mn networks coexist. In region II, the proportion of Mn^{4+} ions increases as the Mn composition increases because Mn^{4+} is dominant in antiferromagnetic $CaMnO_3$. This leads to the monotonic decrease of the average ferromagnetic spin moment of Mn ions by decreasing the ferromagnetic Mn^{3+}–Mn^{4+} pairs. As the proportion of Mn^{3+} ions decreases, the number of Ru^{5+} ions decreases. However, the proportion of Ru^{5+} to Ru^{4+} increases. As a result, the average Ru moment continues to increase (see figure 6). The antiferromagnetic $Mn^{4+} - Mn^{4+}$ pairs can affect the ferromagnetic coupling between Ru ions, which accounts for the saturation of the average spin moment of Ru ions above $x = 0.7$.

Finally, although it possesses a single structural phase over the whole x range, $CaRu_{1-x}Mn_xO_3$ is a magnetically inhomogeneous system which appears between itinerant paramagnetic $CaRuO_3$ and localized antiferromagnetic $CaMnO_3$. The inhomogeneity in the magnetic ground state may be associated with the coexistence of the itinerant and localized natures of the electron system in $CaRu_{1-x}Mn_xO_3$.

4. Conclusion

A magnetic Compton scattering experiment was done for $CaRu_{1-x}Mn_xO_3$ ($0.2 \leqslant x \leqslant 0.9$) to investigate the magnetism by the absolute value of spin moment and magnetic Compton profiles. The doping of Mn introduced a spin magnetic moment on Ru ions and the Ru and Mn spin moments were antiferromagnetically coupled. The average spin moment of Ru ions was proportional to that of Mn ions in the x range. The present experimental result was explained by a mixed valence model and inhomogeneous magnetic structure. Consequently, this experiment suggested that the magnetic ground state in $CaRu_{1-x}Mn_xO_3$ would be an inhomogeneous system, in which the $Mn^{3.5+}$ and $Ru^{4.5+}$ clusters form a ferrimagnetic network in the paramagnetic matrix $CaRuO_3$ for $x < 0.5$ and in the antiferromagnetic matrix $CaMnO_3$ for $x > 0.5$.

Acknowledgments

The work conducted at Aoyama Gakuin University was supported by The Private School High-tech Research Center Program of the MEXT, Japan. The magnetic Compton scattering experiment was performed with the approval of JASRI (J05A08W0–0513N and 2007B1410).

References

[1] Cao G, McCall S, Shepard M, Crow J E and Guertin R P 1997 *Phys. Rev.* B **56** 321
[2] Cao G, Freibert F and Crow J E 1997 *J. Appl. Phys.* **81** 3884
[3] Cao G, McCall S, Bolivar J, Shepard M, Freibert F, Henning P, Crow J E and Yuen T 1996 *Phys. Rev.* B **54** 15144
[4] Hiraoka N *et al* 2004 *Phys. Rev.* B **70** 054420
[5] He T and Cava R J 2001 *Phys. Rev.* B **63** 172403
[6] Sugiyama T and Tsuda N 1999 *J. Phys. Soc. Japan* **68** 1306
[7] Raveau B, Maignan A, Martin C and Hervieu M 2000 *Mater. Res. Bull.* **35** 1579
[8] Maignan A, Martin C, Hervieu M and Raveau B 2001 *Solid State Commun.* **117** 377
[9] Markovich V, Auslender M, Fita I, Puzniak R, Martin C, Wisniewski A, Maignan A, Raveau B and Gorodetsky G 2006 *Phys. Rev.* B **73** 014416
[10] Taniguchi T *et al* 2008 *Phys. Rev.* B **77** 014406
[11] Shames A I, Rozenberg E, Martin C, Maignan A, Raveau B, André G and Gorodetsky G 2004 *Phys. Rev.* B **70** 134433
[12] Terai K *et al* 2007 *J. Magn. Magn. Mater.* **310** 1070

[13] Yoshii K, Nakamura A, Mizumaki M, Tanida H, Kawamura N, Abe H, Ishii Y, Shimojo Y and Morii Y 2004 *J. Magn. Magn. Mater.* **272–276** e609
[14] Felner I, Asaf U, Nowik I and Bradaric I 2002 *Phys. Rev.* B **66** 054418
[15] Koriyama A, Ishizaki M, Ozawa T C, Taniguchi T, Nagata Y, Samata H, Kobayashi Y and Noro Y 2004 *J. Alloys Compounds* **372/1-2** 58–64
[16] Mizusaki S, Hiraoka N, Nagao T, Itou M, Sakurai Y, Taniguchi T, Okada N, Nagata Y, Ozawa T C and Noro Y 2006 *Phys. Rev.* B **74** 052401
[17] Taniguchi T *et al* 2007 *Phys. Rev.* B **75** 024414
[18] Bréard Y, Hardy V, Raveau B, Maignan A, Lin H-J, Jang L-Y, Hsieh H H and Chen C T 2007 *J. Phys.: Condens. Matter* **19** 216212
[19] He T and Cava R J 2001 *J. Phys.: Condens. Matter* **13** 8347
[20] Cooper M J 1985 *Rep. Prog. Phys.* **48** 415
[21] Sakai N 1998 *J. Synchrotron Radiat.* **5** 937
[22] Schmidt M W *et al* 1993 *J. Comput. Chem.* **14** 1347
[23] Taniguchi T, Mizusaki S, Okada N, Nagata Y, Kobayashi Y, Watanabe I, Suzuki T, Ozawa T C, Samata H and Noro Y μSR experiment carried out for single crystal $CaRuO_3$ at 0.3 K, in preparation
[24] Hiraoka N *et al* 2004 *Phys. Rev.* B **70** 054420
[25] Goodenough J B, Woid A, Arnot R J and Menyuk N 1961 *Phys. Rev.* **124** 373
[26] Longo J M, Raccah P M and Goodenough J B 1968 *J. Appl. Phys.* **39** 1327
[27] de Gennes P G 1960 *Phys. Rev.* **118** 141